Colloids and Surfaces A: Physicochem. Eng. Aspects 511 (2016) 135–144

Contents lists available at ScienceDirect

Colloids and Surfaces A: Physicochemical and Engineering Aspects

journal homepage: www.elsevier.com/locate/colsurfa

Dielectric relaxation of suspension of polystyrene-poly (butyl acrylate) (PS-PBA) particles and dielectric model analysis: Electrical and electrokinetic parameters

Mingjuan Han[b], Huarui Wang[a], Jiaoyang Li[a], Kongshuang Zhao[a,*]

[a] College of Chemistry, Beijing Normal University, Beijing, 100875, China
[b] College of Chemistry and Molecular Engineering, Nanjing Tech University, Nanjing, 210009, China

HIGHLIGHTS

- Two-relaxation dielectric behavior of polystyrene-poly (butyl acrylate) (PS-PBA) particles was investigated over the frequency range of 40 kHz to 110 MHz.
- Phase parameters-the extracted individual electrical information of particles and continuous medium were obtained by Hanai method.
- Electrokinetic parameters were obtained on the basis of phase parameters.

GRAPHICAL ABSTRACT

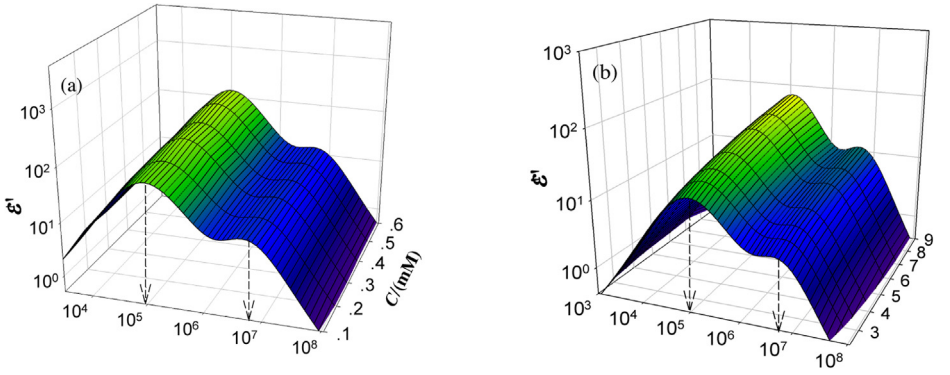

Three-dimensional representations of KCl concentration (a) and mass fraction of PS-PBA particles in suspension (b) dependences of the derivative dielectric loss spectra. Note: They have been processed by eliminating the electrode polarization. The arrows indicated the low- and high- relaxation frequencies.

ARTICLE INFO

Article history:
Received 14 July 2016
Received in revised form
21 September 2016
Accepted 23 September 2016
Available online 23 September 2016

Keywords:
PS-PBA colloidal disperse system
Dielectric relaxation spectroscopy (DRS)
Electrical double layer
Electrokinetic parameters

ABSTRACT

Dielectric behaviors of suspensions of monodisperse polystyrene-poly (butyl acrylate) (PS-PBA) particles with the radius of 120 nm were thoroughly investigated in the frequency range of 40 Hz to 110 MHz. Two remarkable dielectric relaxations were simultaneously observed, and the well-known Einstein equation and Grosse theory were employed to analysis the relaxation mechanism. Meanwhile, Dukhin-Shilov theory about the thin double layer of colloid dispersion was employed to verify the effects of volume fraction and KCl electrolyte concentration on dielectric parameters of DRS. The results showed that the changing trend of relaxation frequencies and dielectric increments from experimental data with KCl concentration and volume fraction was well consistent with the prediction of the wide-range DRS of Dukhin-Shilov theory. In addition, the reasonable phase parameters (ε_p,κ_p,ε_a,$\kappa_a$andϕ) were calculated by Hanai theory on the basis of the suggested dielectric model. Finally, the interfacial electrical parameters (λ,σ,ζ) of PS-PBA microspheres dispersed in different concentrations of KCl electrolyte solution were obtained by electrodynamics equations about interface on the basis of dielectric analysis. More importantly, the calculated value of ζ well agreed with the value (- 48.8 mV) measured by Zeta potential analyzer,

* Corresponding author.
E-mail address: zhaoks@bnu.edu.cn (K. Zhao).

http://dx.doi.org/10.1016/j.colsurfa.2016.09.077
0927-7757/

thus the result proved that DRS was a feasible method to investigate the interfacial electrical parameters of disperse system in a non-intrusive way.

1. Introduction

Colloidal particles as a type of classical soft materials have attracted much attention for their key and potential applications in various fields such as materials [1,2], food [3] and paint [4], especially biomedical applications [5–7]. Up to now, key investigations on colloidal disperse systems were focused on the synthesis of colloidal particles and on their structure properties which were characterized by the method of IR, XRD, TG-DTA, EDS, XPS and TEM, separately. Meanwhile, Dynamic adsorption and characterization at liquid/liquid interfaces for colloidal disperse systems were investigated in detail [8–10]. From the aforementioned investigations, the morphology of colloidal particles and their solid-state structure characteristics, corresponding stability problem, and the process of dynamic adsorption could be obtained. For the aspect of fundamental research and applicable area, the liquid properties and electrical properties of colloidal disperse systems (such as viscosity, conductivity, permittivity et al) and their electrokinetic properties were also important to the stability of colloidal particles in a colloid. In order to evaluate the stability of colloidal disperse system, the electrokinetic phenomena in a static electric field were widely studied, such as electrophoresis, electroosmosis, sedimentation potential and streaming potential, especially electrophoresis [11] was the most widely used one, and has been found that both electrophoretic transport and aggregative stability of suspensions were controlled by the interfacial electric charges, referred to electrical double layer (EDL), at liquid/solid interfaces. Nevertheless, it has been realized that the investigations of only electrokinetic measurements were insufficient to completely characterize the EDL related to the stability of particle suspensions, and then electrokinetic and dielectric properties were often used for the characterization of colloidal systems [12–14]. This was why theoretical models relating these electrokinetic phenomena to the system parameters have been developed in the last century. Therefore, probably the key relevant factors, such as electric and dielectric properties of particle suspensions, should be considered and studied in the electrical analysis on the colloidal stability.

Dielectric Relaxation Spectroscopy (DRS), as one of the important physical methods characterized the physical property, has been very early used to study the disperse system of colloidal particles [15–17], meanwhile, it could provide the information related to the hydrokinetics, and the structure characteristics and electric/dielectric properties of dispersed particles and continuous medium. It was well-known that suspensions could be characterized by mechanisms of two typical relaxations: the low-frequency relaxation (α relaxation) and the high-frequency relaxation (M-W-O relaxation), both of them were sensitive to the polarization of electrical double layer of dispersed particles. As for the low-frequency relaxation, a condensed counterion model (surface diffusion mechanism, SDM) for insulating particles suspended in electrolyte solution was proposed by Schwarz [18] by assuming that counterions only move along the particle surface without exchanging with ions in the bulk electrolyte solution. Then, Dukhin and Shilov [19] proposed a different model that included diffusion of ions in the bulk phase and exchange of ions between the electrical double layer and bulk phase, it was named volume diffusion mechanism, VDM. As for the high-frequency relaxation, O'konski [20] generalized M-W relaxation theory [21] by including a surface conductivity of the particles to calculate of the effective bulk conductivity of a spherical particle, equivalent to the model of dispersed particle consisting of an insulating core and a conducting shell. The theoretical models simultaneously including both relaxations in the wide frequency range were proposed by O'Brien [22] and Grosse [23,24], which gave a simplified treatment of the low-frequency relaxation but with the inclusion of surface conductivity.

On the other hand, based on the O'Brien and White model [16] for a static field, a very important progress in both mechanisms was ascribed to numerical solutions by DeLacey and White [25], who developed the standard model for calculating the complex conductivity of dilute suspensions of non-conducting spheres in an oscillating electric field, but surface conductivity behind the shear plane was not considered. Then, Mangelsdorf and White [17] developed the numerical model of DeLacey White by considering the electrical conductivity behind the slip plane, and calculated the DC conductivity and the electrophoretic conductivity of suspensions. By comparison with numerical results of DeLacey and White, Shilov et al. [26] proposed the well-known results of Dukhin-Shilov theory of thin double layer polarization by taking into account the surface conductivity behind the shear plane. In recent works, particles coated with a permeable membrane (soft particles) have been investigated [27,28], a network model made it possible to obtain readily not only the electrophoretic mobility but also the physical variables related to the suspended particles (electric potential, ion concentrations, fluid velocity).

Correspondingly, the experimental study of DRS lagged behind, and the previous experimental investigation about DRS mainly concentrated on disperse systems of polystyrene [29–31] and SiO_2 spheres [32–34]. And even if the investigated system was the suspension of the typical rigid PS particles, disagreements between theoretical predictions and experimental data on different electrokinetic phenomena based on the DRS were often reported [35,36]. The reasons responsible for the situation were ascribed to two aspects: one was the low-frequency relaxation appeared in kHz frequency range could be covered by electrode polarization (EP), which resulted in that a valuable DRS was difficult to be obtained; the other was the current theoretical analysis has no ability to deal with various colloidal disperse systems. Perhaps just because of these two reasons, there were so few typical two-relaxation systems [24,34] were found in experimental section although the investigators were most interested in their corresponding two-relaxation characterization. As the former drawback, a number of methods have been derived to eliminate the effect of EP on the determination of experimental data [24,37–39], especially the data treatment method such as the logarithmic derivative method [38,39] was widely applied, which was also employed in this work. While the second drawback aforementioned may be overcame by attempting to introduce or develop the more dielectric analysis methods and more experimental disperse systems.

In this work, suspension of PS-PBA particles with the radius of 120 nm was employed as research system and its dielectric measurement was performed over a frequency range of 40 Hz to 110 MHz. The aim of this work is to show a new colloidal disperse system with two-relaxation phenomenon, and subsequent event is to verify the two-relaxation mechanisms proposed by Grosse and the consistency between the existing Dukhin-Shilov theory [26] and experimental data. Meanwhile, an effective method, we called

Hanai method hereafter, was employed, which could accurately relate observed dielectric parameters to phase parameters for a spherical disperse system [40,41], and has been used in various systems [34,42] and proved to be valid and practical. Accordingly, we will take extra steps to obtain the phase parameters (permittivity and conductivity of dispersed particles and continuous medium, respectively, and volume fraction of dispersed particles) on the basis of our developed dielectric model for PS-PBA suspension. In addition, we will show how to obtain the electrical information (such as zeta potential, surface electrical charges and surface conductivity) at liquid/solid interface on the basis of dielectric analysis.

2. Experimental section

2.1. Materials and instruments

Materials: Styrene, butyl Acrylate, acrylic acid, sodium lauryl sulfate, ammonium persulfate, sodium carbonate, KCl and emulsifier Op-10 were AR and manufactured by Beijing chemical factory. Double-distilled water with the conductivity lower than 1.0×10^{-6} S/m was used to prepare solution.

Instruments: Agilent 4294A precision impedance analyzer; Zeta potential analyzer (Malvern Instruments Ltd).

2.2. Preparation of suspensions of PS-PBA particles

First, synthesis of the latex of monodisperse PS-PBA particles: The amount of each chemical medicine was shown in Table S1. First, *D* solution in Table S1 was introduced into 250 mL of ground glass stoppered flask with electric stirring function, and the solution was stirred and heated, then the *C* solution was added into the flask when the temperature reached up to 60 °C. Subsequently, *A* and *B* solutions were gradually added into the flask for 3 h when the temperature was up to 78 °C, and then the reaction needed to continue for 1 h. Finally, impurities in the latex of PS-PBA particles were removed by centrifugal cleaning for 6 times. Then, the synthesized PS-PBA particles were characterized by TEM, as shown in Fig. S1. TEM showed that the radius of PS-PBA microspheres was 120 (±10) nm.

Dialysis treatment of monodisperse PS-PBA particles: (a) Suspensions of PS-PBA particles with different concentrations of KCl electrolyte solution: 6 types of concentrations of KCl electrolyte solution (0.1, 0.2, 0.3, 0.4, 0.5, 0.6 mM) were put in 500 mM of volumetric flask to constant volume, respectively. And then we took out 5 mL from each type and put them into the bag filters, and dialyzed with stirring for 24 h and standing for 24 h in different concentrations of KCl electrolyte solution, respectively. Finally, suspensions of PS-PBA particles were ultrasonic dispersion for 30 min, and then dielectric measurement was carried out by taking out 2 mL from the each bag filter, one by one. (b) Suspensions of PS-PBA particles with different volume fractions in 0.2 mM KCl electrolyte solution: First, suspension of mass fraction 9% of PS-PBA particles were prepared for 7 portions, and then they were diluted with water to 7.2%, 6.0%, 4.5%, 3.6%, 3.0% and 2.3%, respectively. And then we took out 5 mL from each portion and put them into the bag filters, and dialyzed with stirring for 24 h and standing for 24 h in the same concentration (0.2 mM) of KCl electrolyte solution, respectively. Finally, suspensions of PS-PBA particles were ultrasonic dispersion for 30 min, and then dielectric measurement was carried out by taking out 2 mL from the each bag filter, one by one.

2.3. Dielectric measurements

Dielectric measurements of suspensions of PS-PBA particles were performed using a 4294A precision impedance analyzer (Agilent Technologies) over a frequency range from 40 Hz to 110 MHz. The dielectric measuring cell with concentrically cylindrical platinum electrodes was employed [43]. The applied alternating field was 500 mV, and the measurement temperature was 24 ± 0.5 °C.

To eliminate the errors from the residual inductance, the experimental data were corrected by the stray capacitance C_r and cell constant C_l of the permittivity cell, which were determined by using several standard liquids, such as pure water, ethanol and acetone. The residual inductance L_r due to the cell assembly and the terminal leads will make errors, so L_r of the dielectric cell was determined by use of standard KCl solutions with different concentrations. Then, the permittivity and conductivity were calculated from the corrected capacitance and conductance [44].

3. Determination of dielectric parameters and phase parameters of DRS

3.1. Determination of dielectric parameters

Under an AC electric field, the complex permittivity of suspensions of PS-PBA particles could be defined as

$$\varepsilon^*(\omega) = \varepsilon'(\omega) - j\frac{\kappa(\omega)}{\varepsilon_0\omega} = \varepsilon'(\omega) - j\left(\varepsilon''(\omega) + \frac{\kappa_l}{\omega\varepsilon_0}\right) \quad (1)$$

Where $\varepsilon'(\omega)$ and $\kappa(\omega)$ were the frequency-dependent real parts of the complex permittivity and conductivity, respectively, κ_l was the low-frequency limit of conductivity, and $j^2 = -1$. The total dielectric loss contained two parts: the effective dielectric loss of suspension and the low-frequency conductivity. From the Eq. (1), the contribution of the low-frequency conductivity could be subtracted from the conductivity spectra through the equation,

$$\varepsilon''(\omega) = \frac{(\kappa(\omega) - \kappa_l)}{\varepsilon_0\omega} \quad (2)$$

Two remarkable relaxations were observed for all suspensions of PS-PBA microspheres with different KCl concentrations and mass fractions in the range of our investigated frequency. Generally speaking, the following relaxation function including two Cole-Cole's terms and the electrode polarization term $A\omega^{-m}$(A and m are adjustable parameters) was used to analyze the experimental spectra [45],

$$\varepsilon^* = \varepsilon_h + \frac{\varepsilon_l - \varepsilon_{mid}}{1 + (j\omega\tau_l)^{\beta_l}} + \frac{\varepsilon_{mid} - \varepsilon_h}{1 + (j\omega\tau_h)^{\beta_h}} + A\omega^{-m} \quad (3)$$

Where ε_l and ε_h were the low- and high-frequency limits of permittivity; τ_l and τ_h were the characteristic relaxation times of the low- and high-frequency relaxations, respectively. β_l and β_h ($0 < \beta \leq 1$) were the parameters indicating the distribution of relaxation time τ_l and τ_h($\tau = 1/\omega = 1/(2\pi f)$), individually; ω was the angular frequency.

In order to determine the characteristic dielectric parameters (ε_l,ε_m,ε_h, and τ_l,τ_h) more accurately, the dielectric loss ε''_{der} was presented by logarithmic derivative $\varepsilon''_{der} = -(\pi/2)(\partial\varepsilon'/\partial \ln\omega)$on the basis of the logarithmic derivative of raw$\varepsilon'(\omega)$ data. The method has been turned out to be very effective in resolving overlapped relaxations and also in separating relaxations from EP [38,39]. By introducing the real part of Eq. (3) into the equation of ε''_{der}, the following equation was derived,

$$\varepsilon''_{der}(\omega) = \frac{\pi}{2}\left(\sum_i \frac{\beta_i(\Delta\varepsilon_i)(\omega\tau_i)^{\beta_i}\cos\left[\frac{\beta_i\pi}{2} - (1+\beta_i)\theta_i\right]}{1 + 2(\omega\tau_i)^{\beta_i}\cos\frac{\beta_i\pi}{2} + (\omega\tau_i)^{2\beta_i}}\right) \quad (4a)$$

$$\theta_i = \arctan\left[\frac{\sin\left(\frac{\beta_i\pi}{2}\right)}{(\omega\tau_i)^{\beta_i} + \cos\left(\frac{\beta_i\pi}{2}\right)}\right] \quad (4b)$$

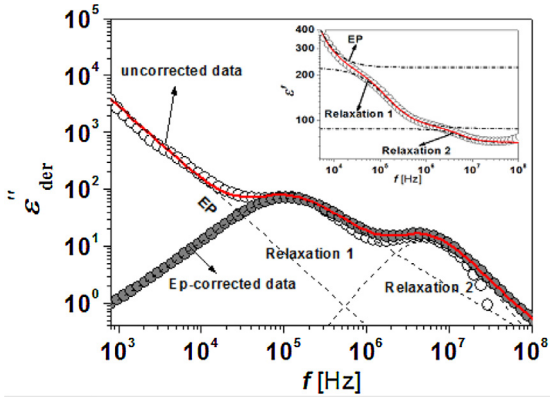

Fig 1. Frequency dependence of the derivative dielectric loss of PS-PBA particles in 0.1 M KCl electrolyte aqueous solution at 24 ± 0.5 °C. The inset showed the fitting result (using Eq. (3)) of the relative permittivity by using the same fitting parameters except for β values as those using Eq. (4) to fit ε''_{der} curves. The hollow circles were the uncorrected data and the solid circles were the corrected curves after subtraction of the EP effect. The red lines and the short dot lines represented the best fitting lines. (For interpretation of the references to colour in this figure legend, the reader is referred to the web version of this article.)

Eq. (4a) has the same set of variables as that in Eq. (3) and was employed to fit the derivative dielectric loss curve in this work.

A simultaneous fit of $\varepsilon'(\omega)$ curves and ε''_{der} curves was performed: First, the raw permittivity $\varepsilon'(\omega)$ curves were fitted by using Eq. (3) to obtain the first set of relaxation parameters. Second, ε''_{der} was obtained on the basis of $\varepsilon'(\omega)$ data, and ε''_{der} curves after subtraction of the EP effect were obtained using Eqs. (4a) and (4b) when A and m were set 0. Then, we fitted the ε''_{der} curves after subtraction of the EP effect on the basis of the first set of relaxation parameters using Eq. (4a), and simultaneously corrected the first set of relaxation parameters. Finally, the corrected set of relaxation parameters was obtained. The results showed that the obtained relaxation parameters from fitting the ε''_{der} curves after subtraction of the EP effect (using Eq. (4a)) have a little different from those from fitting $\varepsilon'(\omega)$ curves (using Eq. (3)), the reason for this was the logarithmic derivative was very sensitive to overlapped relaxations and EP effect (note: the obvious difference was the values of β, which was ascribed to the peaks of ε''_{der} curves more sharpened than those of $\varepsilon'(\omega)$ curves).

Fig. 1 showed the frequency dependences of the permittivity and derivative dielectric loss spectra. The red solid line in derivative dielectric loss spectrum and permittivity spectrum represented the best fitting line with Eqs. (4a) and (3) with the same set of variables except for β values, respectively. Meanwhile, the EP effect, the contributions from the lower (relaxation 1) and higher (relaxation 2) frequency relaxations were displayed by short dot lines in Fig. 1.

3.2. Dielectric model and Hanai equations for phase parameters

When the PS-PBA particles dispersed in KCl electrolyte solution, the disperse system of PS-PBA spheres could be modeled as particle suspensions with complex permittivity ε^* and conductivity K^*, that was, the PS-PBA particles with radius R, and complex permittivity ε^*_p and conductivity K^*_p dispersed in a continuous KCl solution with complex permittivity ε^*_a and conductivity K^*_a, depicted as Fig. 2. The electrical double layer (EDL), where counter-ions prevailed, was existed when PS-PBA spheres were dispersed in KCl electrolyte solution. As shown in Fig. 2, the interface in the magnified sphere contained the diffuse layer and stagnant layer, and its double layer

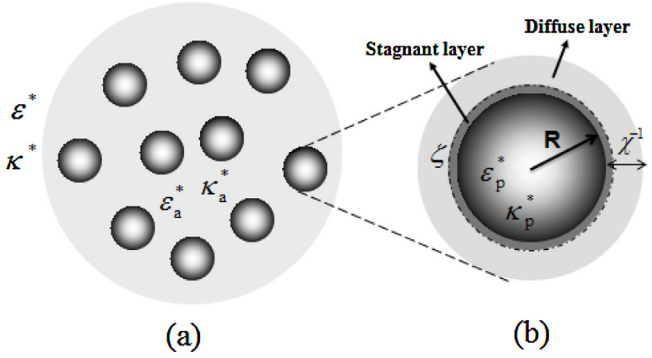

Fig. 2. Schematic diagram of dielectric models (a) PS-PBA suspension and (b) a magnified single PS-PBA sphere.

thickness χ^{-1} (also named the Debye length). χ^{-1} could be calculated from the following equation [26],

$$\chi^{-1} = \sqrt{\frac{\varepsilon_0 \varepsilon_m \kappa T}{2e^2 C_\infty}} \tag{5}$$

Where e the elementary charge, κ the Boltzmann constant, T the absolute temperature, ε_0 the absolute permittivity of vacuum, and ε_m the permittivity of the continuous medium, C_∞ the number concentration of counter-ions or co-ions in the continuous medium. The place between diffuse layer and stagnant layer was the shear plane, where a very important parameter was zeta potential (ζ), which characterized the electrical double layer. The other parameter was surface conductivity κ^σ includes both the surface conductivity within the stagnant layer and the surface conductivity of the diffuse layer beyond the shear plane [26].

Based on the aforementioned dielectric model, the following Hanai mixture equation [46,47], which could accurately relate observed dielectric parameters to phase parameters for a spherical disperse system, could appropriately describe the concentrated PS-PBA suspensions on the basis of the M-W theory,

$$\frac{\varepsilon^* - \varepsilon^*_p}{\varepsilon^*_a - \varepsilon^*_p}\left(\frac{\varepsilon^*_a}{\varepsilon^*}\right)^{1/3} = 1 - \phi \tag{6}$$

Where the subscripts a and p designated the medium and the particle, respectively. In this equation, ϕ was the volume fraction, $\varepsilon^*_p = \varepsilon'_p - j\kappa_p/\omega\varepsilon_0$ and $\varepsilon^*_a = \varepsilon'_a - j\kappa_a/\omega\varepsilon_0$, respectively. Phase parameters (κ_a, ε_p, κ_p and ϕ) described in the model could be approximately calculated from the dielectric parameters using some equations [48] if the permittivity of the medium solution (ε_a) was given. The values of ε_a of varying temperatures could be calculated by the following equation [49],

$$\varepsilon_a(T) = 78.3 \times [1 - 0.004579 \times (T - 25) + 0.0000119 \times (T - 25)^2 - 0.000000028 \times (T - 25)^2] \tag{7}$$

where the measured permittivity of medium ε_a was about 79 at 24 ± 0.5 °C.

Second, as for dilute suspensions, Hanai [40] developed a method to calculate the phase parameters from the dielectric parameters on the basis of the M-W theory,

$$\varepsilon^* = \varepsilon^*_a \frac{2(1-\phi)\varepsilon^*_a + (1+2\phi)\varepsilon^*_p}{(2+\phi)\varepsilon^*_a + (1-\phi)\varepsilon^*_p} \tag{8}$$

Phase parameters (κ_a, ε_p, κ_p and ϕ) determined by dielectric parameters using some equations also could be obtained, which could refer to the article [48].

4. Results and discussion

4.1. Dielectric behaviors of suspensions of PS-PBA particles

Fig. S2 showed the frequency dependences of permittivities for PS-PBA suspensions with different concentrations of KCl solution from 0.1 to 0.6 mM (a) and with different mass fractions from 2.3% to 9.0% (in 0.2 mM KCl solution) (b), respectively. Then, correspondingly, the data of these dielectric loss (ε''_{der}) spectra were obtained according to the logarithmic derivative method, which was described in "Determination of dielectric parameters". Fig. 3 showed dielectric loss (ε''_{der}) spectra after subtraction of the EP effect for suspensions of PS-PBA particles with different KCl concentrations (a) and with different mass fractions (b), respectively. Two remarkable dielectric relaxations were observed at around 10^5 and 10^7 Hz in both Figs. 3a and 3b, called the low- and high-frequency relaxations, respectively. Meanwhile, based on the fitting method dielectric parameters of PS-PBA particles dispersed in different concentrations of KCl solution were displayed in Table 1.

4.2. The mechanisms of low- and high-frequency relaxations

Based on the dielectric parameters shown in Table 1, the mechanisms of low- and high-frequency relaxations could be determined. As well known, the characteristic relaxation time ($\tau = 1/(2\pi f)$) was the most effective criterion to determine the dielectric relaxation mechanism of different types. Here, we introduced the well-known Einstein equation to our analysis for the convenient understanding, $t = \langle x\rangle^2/2D$. $\langle x\rangle$ and D were the average displacement and the average diffusion coefficient of ions, respectively. As for a spherical particle, the characteristic time τ_l of low-frequency relaxation caused by the counter-ion polarization corresponded to the time for the counter-ion to transport from one side of the particle to the other side [31], namely, the transporting distance of counter-ion was $\langle x\rangle \approx 2\left(R+\chi^{-1}\right)$. The characteristic time $\tau_h$of high-frequency relaxation due to the M-W polarization corresponded to the time that counter-ions were shaking back and forth in EDL (as shown in Fig. 2), that was $\langle x\rangle \approx \chi^{-1}$. Therefore, the transporting time of counter-ions corresponding to the two types of relaxations should expressed by $t_l = 4\left(R+\chi^{-1}\right)/2D$ and $t_l = \left(\chi^{-1}\right)^2/2D$, and when the direction of electric field changes and its change of period was equal to the transporting time of counter-ions, namely, the relaxation happened when $t = \pi/\omega(\omega = 2\pi f)$, the relaxation frequency was

$$f_{l,En} = D/[4(R+\chi^{-1})^2] \tag{9a}$$

$$f_{h,En} = D/(\kappa^{-1})^2 \tag{9b}$$

Then, the τ_l and τ_h could be estimated by

$$\tau_{l,En} = \frac{4(R+\chi^{-1})^2}{2\pi D} \tag{10a}$$

$$\tau_{h,En} = \frac{\chi^{-2}}{2\pi D} \tag{10b}$$

D was the ion diffusion coefficient ($D_{(K^+)} \approx D_{(Cl^-)} \approx 2.03\times 10^{-9}m^2s^{-1}$), and R was approximate 120 nm. According to the Eq. (5), χ^{-1} was about 30.4 nm for 1-1 type of 0.1 mM KCl electrolyte solution; $f_{l,En}$ and $f_{h,En}$ were 2.24×10^4 Hz and 2.196×10^6 Hz ($\tau_{l,En} = 7.1\times10^{-6}$ s; $\tau_{h,En} = 7.25\times10^{-8}$ s), which was the same order as those in Table 2. This result showed that the relaxation around the MHz range was the typical M-W-O polarization [20], correspondingly, the relaxation occurring in the kHz frequency range was due to the concentration polarization [19]. Based on the Eqs. (10a) and (10b), $\tau_{h,En}$ and $\tau_{l,En}$ for suspensions of PS-PBA spheres in different concentrations of KCl solution were calculated and displayed in Table 2, their orders of magnitude were also 10^{-6} s and 10^{-8} s, respectively, these orders well coincided with ones of experimental values (shown in Table 2).

Grosse theory [23] was further employed for verifying the relaxation mechanisms.

$$\tau_{\alpha,Gr} = \frac{R^2(D_{K^+}+D_{Cl^-})}{4D_{K^+}D_{Cl^-}} \tag{11a}$$

$$\tau_{\beta,Gr} = \frac{(\varepsilon_p+2\varepsilon_a)\varepsilon_0}{\kappa_p+2\lambda/R+2\kappa_a} \tag{11b}$$

Where the permittivity and conductivity of PS-PBA particles:$\varepsilon_p \approx 5$ and $\kappa_p \approx 0$; λ (-9.0×10^{-11} S) was the surface conductivity of particles; ε_a and κ_a were the permittivity and conductivity of the continuous medium, respectively. According to Eqs. (11a) and (11b), $\tau_{\alpha,Gr}$ and $\tau_{\beta,Gr}$ were calculated, and displayed with $\tau_{h,En}$ and $\tau_{l,En}$ in Table 2 and together with the experimental relaxation time τ_l and τ_h. The results proved the two remarkable relaxations in kHz and MHz frequency ranges were α relaxation and β relaxation (also named M-W-O relaxation) in Grosse theory, respectively, and their relaxation mechanisms were well consistent with ones derived from the transporting theory described by Einstein equation.

Here, first it should be noted that the analysis of τ_l and τ_h for suspensions of PS-PBA particles with different mass fractions (%) could be seen as the sample of 0.2 mM KCl in Table 2 because all investigated PS-PBA particles with different mass fractions were dispersed in 0.2 mM KCl solution. Second, surface conductivity λ obtained by Grosse theory (the following Eq. (14) in this work) was introduced in Table 2, and the reason was that it was necessary for calculating the value of $\tau_{\beta,Gr}$.

4.3. A theoretical simulation to analysis the dielectric parameters

In order to verify the characteristic of relaxation parameters from experimental data, we introduced the Shilov-Dukhin theory [26] (detail in supporting information) to analyze the relaxation parameters of the low- and high-frequency dielectric relaxations. On the basis of the theoretical hypothesis, disperse particles were supposed as non-conducting microspheres compared with the continuous medium, and $\chi R \geq 1$, which were similar to our research system, and dielectric model of suspension of spherical particles could refer to Fig. 2. According to the Shilov-Dukhin theory, the full electric response of disperse system could be considered as functions of the frequency$f$, and characterized by its complex permittivity $\varepsilon^*(\omega)$ and complex conductivity $K^*(\omega)$, respectively, under AC field.

Mathcad procedure, which possessed the special advantage in treating the evaluation of complex functions [50], was used to treat the Eqs. (S3-5). Considering the characteristic of PS particles was well understood, so we chose to simulate the relations between dielectric behavior and electrolyte concentrations/volume fraction of suspensions of PS spheres in KCl solution by Shilov-Dukhin theory [26] to compare with those of PS-PBA suspensions. Table S2 showed the parameters used in computer simulation and the simulation results were shown in Fig. 4. In order to further and clearly investigate the relaxation parameters of DRS for suspensions of PS-PBA particles, the experimental data (in Fig. 5) were extracted from the data in Fig. 3 and showed in two-dimensional representations. Both spectra of derivative dielectric loss$\varepsilon''(\omega)$in Figs. 4 and 5 clearly showed two remarkable dielectric relaxations.

First, from the experimental data in Fig. 5a, we could see that characteristic relaxation frequency f_l of the low-frequency relaxation almost did not change with increasing the KCl electrolyte concentration, but f_h of the high-frequency relaxation slightly shifted to the higher frequencies. The phe-

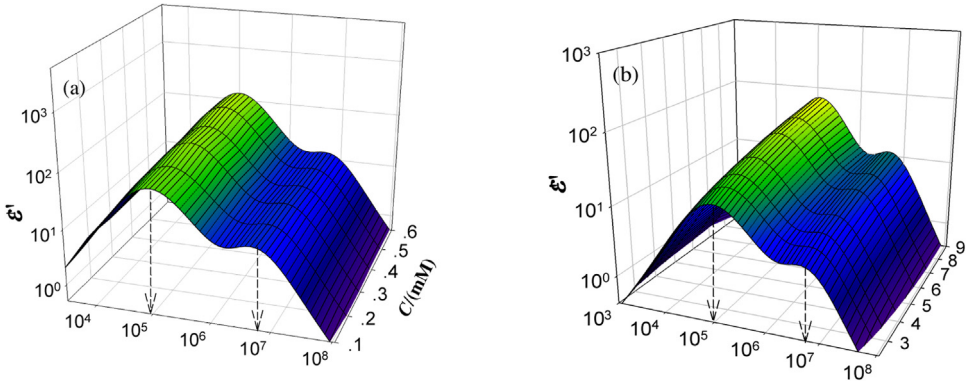

Fig. 3. Three-dimensional representations of KCl concentration (a) and mass fraction of PS-PBA particles in suspension (b) dependences of the derivative dielectric loss spectra. Note: They have been processed by eliminating the electrode polarization. The arrows indicated the low- and high- relaxation frequencies.

Table 1
Dielectric parameters for PS-PBA suspensions of different concentrations of KCl solution (a) and different mass fractions (M%) of PS-PBA particles dispersed in 0.2 mM KCl solution (b).

(a)	KCl (mM)	$\chi^{-1}(\times 10^{-8}$ m)	ε_l	ε_m	ε_h	$\Delta\varepsilon_l$	$\Delta\varepsilon_h$	$\tau_l(\times 10^{-6}$ s)	$\tau_h(\times 10^{-8}$ s)
	0.1	3.04	225	87.5	71.0	138	16.5	1.5924	3.1223
	0.2	2.15	245	86.5	71.0	159	15.5	1.6762	3.0045
	0.3	1.76	275	86.0	70.2	189	15.8	1.6084	2.8952
	0.4	1.52	275	86.0	71.0	189	15.0	1.6587	2.8435
	0.5	1.36	305	85.0	70.4	220	14.6	1.6587	2.7936
	0.6	1.36	305	85.0	70.4	220	14.6	1.6587	2.7936
(b)	M%								
	9.0	2.15	200	86.5	73.5	114.0	13.0	1.4744	3.1407
	7.2	2.15	182	84.2	73.9	97.8	10.0	1.5165	3.0980
	6.0	2.15	166	83.8	74.6	82.2	9.2	1.5311	3.0980
	4.5	2.15	146	83.4.	75.8	62.6	7.6	1.5611	3.0920
	3.6	2.15	134	82.5	76.4	51.5	6.1	1.5924	3.0920
	3.0	2.15	126	81.8	76.7	44.2	5.1	1.5924	3.0860
	2.3	2.15	116	81.1	77.1	34.9	4.0	1.6084	3.0860

Table 2
Comparisons of relaxation times obtained from experimental DRS, Einstein function and Grosse theory.

Fundamental parameters			Relaxation time					
KCl (mM)	$\chi^{-1}(\times 10^{-8}$ m)	$\lambda(\times 10^{-11}$ S)	$\tau_l(\times 10^{-6}$ s)	$\tau_h(\times 10^{-8}$ s)	$\tau_{l,En}(\times 10^{-6}$ s)	$\tau_{h,En}(\times 10^{-8}$ s)	$\tau_{\alpha,Gr}(\times 10^{-6}$ s)	$\tau_{\beta,Gr}(\times 10^{-8}$ s)
0.1	3.04	−9.01	1.5924	3.1223	7.0974	7.2492	3.5734	8.7454
0.2	2.15	−9.72	1.6762	3.0045	6.2823	3.6260	3.5734	8.8095
0.3	1.76	−18.4	1.6084	2.8952	5.9408	2.4298	3.5734	9.6651
0.4	1.52	−16.1	1.6587	2.8435	5.7353	1.8123	3.5734	9.4209
0.5	1.36	−21.0	1.6587	2.7936	5.6003	1.4509	3.5734	9.9517
0.6	1.36	−21.0	1.6587	2.7936	5.6003	1.4509	3.5734	9.9517

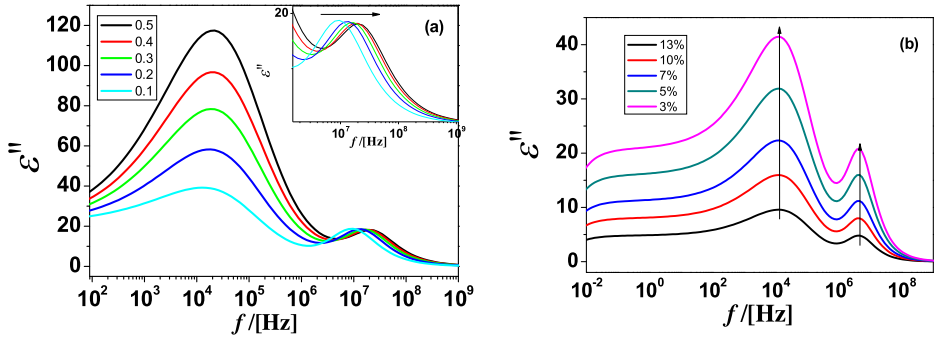

Fig. 4. Frequency dependences of derivative dielectric loss $\varepsilon''(\omega)$ for particles with different KCl electrolyte concentrations (a) and different mass fractions (%) of PS-PBA particles in 0.2 mM KCl solution (b). Note: The spectra are simulation spectra.

nomenon could be explained by $f_{l,En} = D/[4(R+\chi^{-1})^2]$ and $f_{h,En} = D/(\chi^{-1})^2$ expression derived from Einstein equation. From the aforementioned equation, we knew that f_l was the function of both R and χ^{-1}, $\chi R \geq 1$, and then f_l could not obviously change. But, f_h was only the function of χ^{-1}, and χ^{-1} decreased with the increment of KCl electrolyte concentration (as shown in Table 1), then

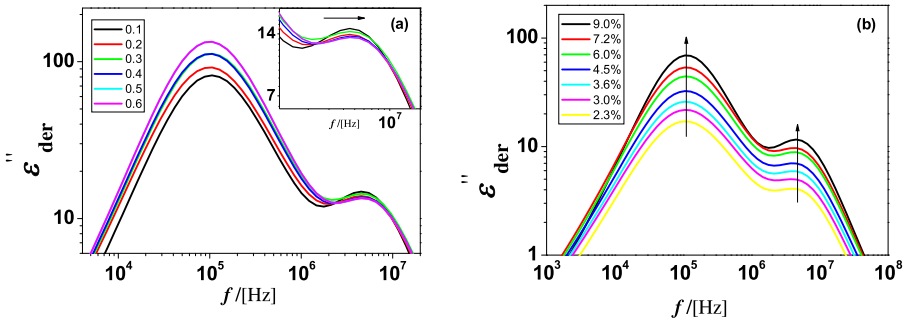

Fig. 5. Frequency dependences of derivative dielectric loss $\varepsilon''(\omega)$ for PS-PBA suspensions with different KCl electrolyte concentrations (a) and different mass fractions (%) of PS-PBA particles in 0.2 mM KCl solution (b). Note: The spectra are extracted from experimental data (in Fig. 3).

f_h decreased according to the direction of Eq. (9b). Meanwhile, it was clearly observed from Fig. 5b that both f_l and f_h did not change with the volume fraction ϕ, and the fact was reasonable because PS-PBA microspheres with different volume fractions were dispersed in the same KCl concentration (0.2 mM) solution, and then it indicated the D and χ^{-1}were almost constants. So, we could conclude both f_l and f_h did not change with the mass fraction (similar to volume fraction) according to Einstein equation. All these phenomena shown in Fig. 5 were in good agreement with ones of theoretical simulation results in Fig. 4.

Second, it was clearly observed from Fig. 5a (the precise data were shown in Table 1) that dielectric increments$\Delta\varepsilon_l$ of the low-frequency relaxation greatly increased with increasing the KCl electrolyte concentration, otherwise, the $\Delta\varepsilon_h$of high-frequency almost did not change (in fact, it increased a little, the precise values were shown in Table 1). The reason for this phenomenon was: $\Delta\varepsilon_l$ was determined by R and the ion concentration of electric double layer [19,24], in fact, $\Delta\varepsilon_l$ is directly proportional to the square root of ion concentration, so $\Delta\varepsilon_l$ increased with the increment of KCl concentration. However, $\Delta\varepsilon_h$ was dominated by the number of polarized charges on the interface andχ^{-1}, as mentioned above, χ^{-1} decreased with the increment of KCl electrolyte concentration although the ion concentration in electric double layer increased, therefore, $\Delta\varepsilon_h$ decreased with the increment of KCl electrolyte concentration. Meanwhile, the dielectric increments were also influenced by the particle volume fraction. Fig. 5b showed that dielectric increments ($\Delta\varepsilon_l$ and $\Delta\varepsilon_h$) of the low- and high-frequencies for suspensions of PS-PBA microspheres greatly increased with increasing the PS-PBA mass fraction, respectively, which was due to the superposition of the long-range electric field of the more polarized particles and their electric double layer, just as the prediction of the Dukhin-Shilov theory (shown in Fig. 4).

4.4. Analysis on phase parameters

According to the dielectric model in Fig. 2 and Hanai theoretical equations, the phase parameters of suspensions of PS-PBA particles were calculated and shown in Table 3. ε_p and κ_p were the permittivity and conductivity of PS-PBA particles, separately. κ_a and ε_a was the conductivity of continuous medium, where $\varepsilon_a$was calculated as 79 at 24±0.5 °C according to Eq. (7).

First, based on Table 3, it was clearly observed that $\varepsilon_p(\varepsilon_p \approx 40)$ of PS-PBA particles dispersed in KCl electrolyte solution were much larger than the one ($\varepsilon_{PS\text{-}PBA,dry\ state} \approx 5$) of dry PS-PBA particles (defined as$\varepsilon_{PS\text{-}PBA}$in the following discussion). The reason for this was: the structure of PS-PBA spheres was loose, hydrophilic groups existed in its structure, especially, both SO_4^{2-} andCOO^- groups were rich in its surface layer of structure, which was much different with the one of rigid PS spheres. If the dry PS-PBA spheres were dispersed in water or electrolyte solution, the water molecules or KCl electrolyte could penetrate into the inner of PS-PBA spheres due to the hydrophilicity of hydrophilic groups. Therefore, the permitivities of wet and dry PS-PBA spheres were much different with each other.

The contribution of water on the permittivity of PS-PBA particles in suspensions could be eliminated [51] by the expression of

$$\varepsilon_p = f_w\varepsilon_w + (1 - f_w)\varepsilon_{PS\text{-}PBA,dry\ state} \tag{12}$$

Where$f_w$was the maximal volume fraction of water penetrated into the inner of PS-PBA spheres, and the calculated values of $f_w$were in the range of 20% – 40%, the permitivities $\varepsilon_p$of PS-PBA microspheres in KCl electrolyte solution were much larger than the ones $\varepsilon_{PS\text{-}PBA,dry\ state} \approx 5$ of dry PS-PBA spheres, meanwhile they were much lower than the permittivity of water ($\varepsilon_{H_2O} \approx 79$). According to this analysis, it could conclude that the calculated $\varepsilon_p$values of PS-PBA spheres were reasonable.

Second, each of the conductivities κ_p of PS-PBA spheres dispersed in KCl electrolyte solution was one order lager than those of κ_a, as shown in Table 3. Two reasons could explain the phenomenon: one reason was the structure of PS-PBA microspheres was loose. Except for the hydrophilic groups (both SO_4^{2-} andCOO^- groups) were rich in its surface layer of structure, meanwhile, the water molecules or KCl electrolyte could penetrate into the inner of PS-PBA spheres and could stay in the pore canals and contribute their conductivity to the whole conductivity $\kappa_p$of particles under AC field. The other reason was although the conductivity of dry PS-PBA spheres was close to zero ($\kappa_{p,dry\ state} \approx 0$), however, actually, the obtained κ_p contained the effective conductivity κ_{eff} of PS-PBA spheres in KCl solution under AC field, and κ_{eff} could be calculated by means of O'Konski equation [20],

$$\kappa_{eff} = \kappa_{p,dry\ state} + \frac{2\lambda}{R} \tag{13}$$

Because $\kappa_{p,dry\ state}$of dry PS-PBA particle equal to 0 ($\kappa_{p,dry\ state} \approx 0$), $\kappa_{eff} = 2\lambda/R$ whereλ was surface conductivity, and its values (shown in the following Table 5) could be obtained by the following Eq. (14) on the basis of dielectric increments ($\Delta\varepsilon_h = \varepsilon_h - \varepsilon_m$, shown in Table 1) and phase parameters (ε_p,κ_p,ε_a,$\kappa_a$andϕ, shown in Table 3) [20].

$$\Delta\varepsilon_h = 9\phi\frac{[\varepsilon_p\kappa_a - \varepsilon_a(\kappa_p + 2\lambda/R)]^2}{(\varepsilon_p + 2\varepsilon_a)(\kappa_p + 2\lambda/R + 2\kappa_a)^2} \tag{14}$$

Therefore, κ_{eff} for PS-PBA spheres in different KCl electrolyte concentrations could be calculated when R was considered as 120 nm), and shown in Table 4 together with the conductivityκ_p (data were extracted from Table 3) calculated from Hanai method. It could be obviously observed from Table 4 that κ_{eff} was only smaller one order than that of κ_a, it indicated that the conductivityκ_{eff} was the main contribution for κ_p.

Table 3
Debye length and Phase parameters for PS-PBA suspensions of different concentrations of KCl solution (a) and different mass fractions (M%) of PS-PBA particles dispersed in 0.2 mM KCl solution (b).

(a)	KCl (mM)	χ^{-1}($\times 10^{-8}$ m)	ϕ(vol.)	κ_a($\times 10^{-3}$ S/m)	ε_p	κ_p($\times 10^{-3}$ S/m)
	0.1	3.04	0.109	7.02	21.9	40.1
	0.2	2.15	0.108	7.71	21.7	40.6
	0.3	1.76	0.133	9.12	26.0	41.3
	0.4	1.52	0.128	9.43	28.5	43.0
	0.5	1.36	0.154	10.8	32.8	42.2
	0.6	1.36	0.154	10.8	32.8	42.2
(b)	(M%)					
	9.0	2.15	0.084	6.76	27.1	42.4
	7.2	2.15	0.068	7.22	21.6	40.2
	6.0	2.15	0.058	6.90	20.8	41.0
	4.5	2.15	0.047	6.16	26.1	40.1
	3.6	2.15	0.037	5.81	24.0	39.1
	3.0	2.15	0.029	5.74	18.8	39.6
	2.3	2.15	0.022	5.63	16.0	37.7

Table 4
The effective conductivity calculated from Eqs. (13) and (14) and the conductivity calculated from Hanai method for PS-PBA particles in different concentrations of KCl solution. Note: $\kappa_p$data in this table contained the κ_p of PS-PBA particles with different mass fractions, which because all PS-PBA particles were dispersed in 0.2 mM KCl electrolyte solution.

Electrolyte (KCl) concentration (mM)	0.1	0.2	0.3	0.4	0.5	0.6
Conductivity κ_p ($\times 10^{-3}$ S/m)	40.1	40.6	41.3	43.0	42.2	42.2
Effect conductivityκ_{eff} ($\times 10^{-4}$ S/m)	15.0	16.0	31.0	26.8	35.0	35.0

Table 5
Interfacial electrical parameters of PS-PBA particles dispersed in different concentrations of KCl electrolyte solution. χ^{-1}Debye length;λ surface conductivity; σ surface charge density; ζ Zeta potential.

KCl (mM)	χ^{-1} ($\times 10^{-8}$ m)	χR	Interfacial electrical parameters					
			First group values			Second group values		
			λ ($\times 10^{-9}$ S)	σ ($\times 10^{-2}$C/m^2)	ζ(V)	λ ($\times 10^{-11}$ S)	σ ($\times 10^{-3}$C/m^2)	ζ(V)
0.10	3.04	3.95	−2.68	−3.52	−0.213	−9.01	−1.18	−0.046
0.20	2.15	5.58	−2.73	−3.48	−0.196	−9.72	−1.28	−0.037
0.30	1.76	6.82	−2.79	−3.66	−0.186	−18.4	−2.42	−0.053
0.40	1.52	7.89	−2.89	−3.79	−0.180	−16.1	−2.11	−0.042
0.50	1.36	8.82	−2.83	−3.71	−0.174	−21.0	−2.76	−0.048
0.60	1.36	8.82	−2.83	−3.71	−0.174	−21.0	−2.76	−0.048

4.5. Calculation of electric parameters of surface of PS-PBA particles

Surface conductivity λ: The well-known Einstein equation and wide-frequency theory of Grosse on DRS have been employed to analysis the relaxation mechanisms in Grosse theory [23] gave the relationship among dielectric increments ($\Delta\varepsilon_h = \varepsilon_h - \varepsilon_m$) and phase parameters ($\varepsilon_p$,$\kappa_p$,$\varepsilon_a$,$\kappa_aand\phi$) and λ, as discussed above in Eq. (14). Therefore, the λ could be calculated (shown in Table 5).

Surface charge densityσ: In the theory of M-W interface polarization, charge density$\sigma$of particle surface and it surface conductivity λ had the direct relation [52],

$$\sigma = \frac{\lambda}{e^2 u} \tag{15}$$

where e was the charge of counter-ion; σ was the charge density of particle surface; u was the ion mobility of counter-ion. Therefore, σcould be calculated (shown in Table 5) according to parameters (e,σ, u and the calculatedλ).

Zeta potential ζ: In the theory of M-W interface polarization, ζ potential could be obtained on the basis of σ and other parameters of electric double layer [53],

$$\sigma = \frac{4C_e e}{\chi} \sinh\left(\frac{e\zeta}{2kT}\right) \tag{16}$$

C_e was the electrolyte concentration; $\chi$was reciprocal of Debye length,

$$\chi^{-1} = \left(\frac{\varepsilon_0 \varepsilon_w kT}{e^2 \sum_i C_i z_i^2}\right)^{1/2} \tag{17}$$

C_i andz_i were the concentration and electric quantity of the i ion, respectively. Thus, the surface conductivity, surface charge density and Zeta potential could be calculated from Eqs. (14)–(17).

Here, it should be noted that two groups of electric parameters for suspension of PS-PBA microspheres were displayed in Table 5. The reason for this phenomenon was due to a quadratic equation (Eq. (14)) with one unknown. From Table 5, we could see that ζ data shown in the first group values were all larger than −100 mV, however, the second group values were in the range of 37–53 mV which was very close to the values (−48.8 mV) measured by Zeta potential analyzer (detail in Supporting information). This showed the second interfacial electric parameters including ζ, which were calculated by electrodynamics equations of interface on the basis of dielectric analysis, were reasonable and reliable.

5. Conclusions

In the work, we showed a new colloidal disperse system (PS-PBA particles in KCl electrolyte) possessed a distinct two-relaxation phenomenon. Two distinct relaxations, at the frequencies $f_l \approx 10^5$ Hz and $f_h \approx 10^7$ Hz, were ascribed to the counter-ion polarization and M-W interface polarization, respectively, which have been confirmed by the well-known Einstein equation and Grosse theory. The dielectric parameters were obtained by using the Cole-Cole equation with two-relaxation terms and EP term to fit the DRS data. Meanwhile, the consistency of experimental DRS data between the prediction of Dukhin-Shilov theory was displayed and analyzed in detail.

DRS reflected the whole dielectric behavior of suspensions and how to extract the individual contribution of particles and continuous medium (phase parameters) was a problem. Compared with the classical articles, the paper at hand addressed how to extract the individual electrical information of particles (phase parameters) from the corresponding dielectric parameters by Hanai method, and the results showed that the calculated phase parameters were reasonable, and we gave the logical explanations.

In addition, we showed that how we used the extracted individual electrical information of particles and continuous phase to calculate the interfacial electrical parameters (λ,σ,ζ) of PS-PBA particles. The results showed that the obtained interfacial parameters were reasonable, more importantly, the calculated zeta potential values were well consistent with the zeta potential value measured by Zeta potential analyzer. This analysis added a new sample to experimental cases for the study of DRS, and provided a feasible method to investigate the interfacial electrical parameters of disperse system in a non-intrusive way.

Acknowledgements

This work is supported by the National Natural Scientific Foundation of China (No. 21173025, 21473012, 21003074), the Major Research Plan of NSFC (21233003) and the Natural Science Foundation of Jiangsu Province (BK20131407).

Appendix A. Supplementary data

Supplementary data associated with this article can be found, in the online version, at http://dx.doi.org/10.1016/j.colsurfa.2016.09.077.

References

[1] S. Sacanna, W.T.M. Irvine, P.M. Chaikin, D.J. Pine, Lock and key colloids, Nature 464 (2010) 575–578.
[2] S.H. Kim, A.D. Hollingsworth, S. Sacanna, S.J. Chang, G. Lee, P. Pine, G.R. Yi, Synthesis and assembly of colloidal particles with sticky dimples, J. Am. Chem. Soc. 134 (2012) 16115–16118.
[3] E. Dickinson, Food emulsions and foams: stabilization by particles, Curr. Opin. Colloid Interface Sci. 15 (2010) 40–49.
[4] B. Ingham, S. Dickie, H. Nanjo, M. Toney, In situ USAXS measurements of titania colloidal paint films during the drying process, J. Colloid Interface Sci. 336 (2009) 612–615.
[5] D.A. Giljohann, D.S. Seferos, W.L. Daniel, M.D. Massich, P.C. Patel, C.A. Mirkin, In vitro selection of structure-switching signaling aptamers, Angew. Chem. Int. Ed. 49 (2010) 3280–3294.
[6] A.S. Dukhin, Z.R. Ulberg, V.I. Karamushka, T.G. Gruzina, Peculiarities of live cells' interaction with micro- and nanoparticles, Adv. Colloid Interface Sci. 159 (2010) 60–71.
[7] Y. Yang, X.H. Yan, Y. Cui, Q. He, D.X. Li, A.H. Wang, J.B. Fei, J.B. Li, Preparation of polymer-coated mesoporous silica nanoparticles used for cellular imaging by a graft-from method, J. Mater. Chem. 18 (2008) 5731–5737.
[8] J.B. Li, G. Kretzschmar, H. Motschmann, R. Miller, H. Möhwald, Characterisation of phospholipid layers at liquid interfaces 3 Relaxation of spreading phospholipid monolayers under harmonic area changes, Colloids Surf. A 114 (1996) 277–285.
[9] Q. He, Y. Zhang, G. Lu, R. Miller, H. Möhwald, J.B. Li, Dynamic adsorption and characterization of phospholipid and mixed phospholipid/protein layers at liquid/liquid interfaces, Adv. Colloid Interface Sci. 140 (2008) 67–76.
[10] J.B. Li, R. Miller, H. Möhwald, Characterisation of phospholipid layers at liquid interfaces. 1. Dynamics of adsorption of phospholipids at the chloroform/water interface, Colloids Surf. A 114 (1996) 113–121.
[11] C. Felix, A. Yaroshchuk, S. Pasupathi, B.G. Pollet, M.P. Bondarenko, V.I. Kovalchuk, E.K. Zholkovskiy, Electrophoresis and stability of nano-colloids: history: theory and experimental examples, Adv. Colloid Interface Sci 211 (2014) 77–92.
[12] R.J. Hunter, Foundations of Colloid Science, vol. I, Oxford University Press, London, 1995.
[13] J. Lyklema, Fundamentals of colloid and interface science Solid/Liquid Interface, vol.II, Academic Press, London, 1995.
[14] M.L. Jiménez, F.J. Arroyo, F. Carrique, A.V. Delgado, Surface conductivity of colloidal particles: experimental assessment of its contributions, J. Colloid Interface Sci. 316 (2007) 836–843.
[15] P.H. Wiersema, A.L. Loeb, J. Th G. Overbeeck, Calculation of the electrophoretic mobility of a spherical colloid particle, J. Colloid Interface Sci. 22 (1966) 78–99.
[16] R.W. O'Brien, L.R. White, Electrophoretic mobility of a spherical colloidal particle, J. Chem. Soc. Faraday Trans. 2 (74) (1978) 1607–1626.
[17] C.S. Mangelsdorf, L.R. White, Effects of stern-layer conductance on electrokinetic transport properties of colloidal particles, J. Chem. Soc. Faraday Trans. 86 (1990) 2859–2870.
[18] G. Schwarz, A theory of the low-frequency dielectric dispersion of colloidal particles in electrolyte solution, J. Phys. Chem. 66 (1962) 2636–2642.
[19] S.S. Dukhin, V.N. Shilov, Dielectric Phenomena and the Double Layer in Dispersed Systems and Polyelectrolytes, Wiley, New York, 2016, pp. 1974.
[20] C.T. O'konski, Electric properties of macromolecules. V. Theory of ionic polarization in polyelectrolytes, J. Phys. Chem. 64 (1960) 605–615.
[21] K.W. Wagner, Erklärung der dielektrischen Nachwirkungsvorgänge suf Grund Maxwellscher VorstellungenErklärung der dielektrischen nachwirkungsvorgänge suf grund maxwellscher vorstellungen, Arch. Electrotech. 2 (1914) 371–387.
[22] R.W. O'Brien, The high-frequency dielectric dispersion of a colloid, J. Colloid Interface Sci. 113 (1986) 81–93.
[23] C. Grosse, Permittivity of a suspension of charged spherical particles in electrolyte solution. 2. Influence of the surface conductivity and asymmetry of the electrolyte on the low- and high-frequency relaxations, J. Chem. Phys. 92 (1988) 3905–3910.
[24] J.D. Solier, R. Roldán-Toro, Wide-frequency-range dielectric response of polystyrene latex dispersions, J. Colloid Interface Sci. 274 (2004) 76–88.
[25] L.R. White, E.H.B. DeLacey, Dielectric response and conductivity of dilute suspensions of colloidal particles, J. Chem. Soc. Faraday Trans. 2 (77) (1981) 2001–2039.
[26] A.V. Delgado, V.N. Shilov, C. Grosse, F. Gonzalez-Caballero, Thin double layer theory of the wide-frequency range dielectric dispersion of suspensions of non-conducting spherical particles including surface conductivity of the stagnant layer, Colloids Surf. A 192 (2001) 253–265.
[27] C. Grosse, J.J. López-García, J. Horno, Numerical study of colloidal suspensions of soft spherical particles using the network method: 2. AC electrokinetic and dielectric properties, J. Colloid Interface Sci. 265 (2003) 341–350.
[28] J.J. López-García, C. Grosse, J. Horno, Analysis of the response of suspended colloidal soft particles to a constant electric field, J. Colloid Interface Sci. 286 (2005) 400–409.
[29] P.V. Christensen, K. Keiding, The use of dielectric spectroscopy for the characterization of the precipitation of hydrophobically modified poly(acrylic-acid) with divalent barium ions, J. Colloid Interface Sci. 340 (2009) 46–52.
[30] A.D. Hollingsworth, D.A. Saville, Dielectric spectroscopy and electrophoretic mobility measurements interpreted with the standard electrokinetic model, J. Colloid Interface Sci. 272 (2004) 235–245.
[31] M. Tirado, C. Grosse, Dependence of the broad frequency dielectric spectra of colloidal polystyrene particle suspensions on the difference between the counterion and co-ion diffusion coefficients, J. Colloid Interface Sci. 298 (2006) 973–981.
[32] L.A. Rosen, D.A. Saville, Dielectric spectroscopy of colloidal dispersions: comparisons between experiment and theory, Langmuir 7 (1991) 36–42.
[33] J. Van Kijlstra, H.P. Leeuwen, J. Lyklema, Low-frequency dielectric relaxation of hematite and silica sols, Langmuir 9 (1993) 1625–1633.
[34] K.S. Zhao, K.J. He, Dielectric relaxation of suspensions of nanoscale particles surrounded by a thick electric double layer, Phys. Rev. B 74 (2006) 205319.
[35] S.J. Miklavcic, B.H. Bradshaw-Hajek, L.R. White, Dynamic dielectric response of concentrated colloidal dispersions comparison between theory and experiment, Langmuir (25 2009) 1961–1969.
[36] P.J. Beltramo, R. Roa, F. Carrique, E.M. Furst, Dielectric spectroscopy of concentrated colloidal suspensions, J. Colloid Interface Sci. 408 (2013) 54–58.
[37] P.A.M. Steeman, J. Van Turnhout, A numerical Kramers-Kronig transform for the calculation of dielectric relaxation losses free from Ohmic conduction losses, Colloid Polym. Sci. 275 (1997) 106–115.
[38] M.L. Jiménez, F.J. Arroyou, J.V. Turnhout, A.V. Delgado, Analysis of the dielectric permittivity of suspensions by means of the logarithmic derivative of its real part, J. Colloid Interface Sci. 249 (2002) 327–335.
[39] J.M. Wübbenhorst, J. Van Turnhout, Conduction-free dielectric loss –a powerful tool for the analysis of strong (ion) conducting dielectric materials, Dielectr. Newsl. 11 (2000) 1–6.

[40] T. Hanai, A. Ishikawa, N. Koizumi, Systematic analysis to determine the dielectric phase, Bull. Inst. Chem. Res. Kyoto Univ. 55 (1977) 376–393.
[41] T. Hanai, T. Imakita, N. Koizumi, Analysis of dielectric relaxations of W/O emulsions in the light of theories of interfacial polarization, Colloid Polym. Sci. 260 (1982) 1029–1034.
[42] Z. Chen, K.S. Zhao, Dielectric analysis of macroporous anion-exchange resin beads suspensions, J. Colloid Interface Sci. 276 (2004) 85–91.
[43] T. Hanai, H.Z. Zhang, K. Sekine, K. Asaka, K. Asami, The number of interfaces and the associated dielectric relaxations in heterogeneous systems, Ferroelectrics 86 (1988) 191–204.
[44] K. Asami, A. Irimajiri, T. Hanai, N. Koizumi, A method for estimating residual inductance in high frequency A.C. measurements, Bull. Inst. Chem. Res. Kyoto Univ. 51 (1973) 231–245.
[45] K.S. Cole, R.H. Cole, Dispersion and absorption in dielectrics I. Alternating current characteristics, J. Chem. Phys. 9 (1941) 341–351.
[46] T. Hanai, Theory of the dielectric dispersion due to the interfacial polarization and its application to emulsions, Kolloid Z. 171 (1960) 23–31.
[47] T. Hanai, A remark on the Theory of the dielectric dispersion due to the interfacial polarization, Kolloid Z. 175 (1961) 61–62.
[48] M.J. Han, K.S. Zhao, Dielectric behavior of suspensions of polystyrene-zinc oxide composite microspheres, J. Phys. Chem. C 112 (2008) 9192–9202.
[49] D.R. Lide, CRC Handbook of Chemistry and Physics, CRC Press, Boca Raton, Florida, 2000.
[50] Y. Lin, Z. Song, Introduction of Mathcad 7.0 and Application in Engineering, Publishing House of People's Post and Tele, Beijing, 1999 (in Chinese).
[51] K.S. Zhao, K. Asami, J.P. Lei, Dielectric analysis of chitosan microsphere suspensions: study on its ion adsorption, Colloid. Polym. Sci. 280 (2002) 1038–1044.
[52] S. Takashima, Electrical Properties of Biopolymers and Membranes, Adam Hilger, Bristol and Philadelphia, 1989, pp. 173–183.
[53] S. Pedrosa, C. Grosse, V.N. Shilov, On the influence of size, (potential, and state of motion of dispersed particles on the conductivity of a colloidal suspension, J. Colloid Interface Sci. 251 (2002) 304–310.